Multi-Wavelength Visible Light Communication System Design

Pankil M. Butala, Hany Elgala, Thomas D.C. Little
Department of Electrical and Computer Engineering
Boston University, Boston, MA, USA
{pbutala, helgala, tdcl}@bu.edu

Payman Zarkesh-Ha
Department of Electrical and Computer Engineering
University of New Mexico, Albuquerque, NM, USA
payman@ece.unm.edu

Visible light communications are achieved by modulation of one or more spectral components in the visible spectrum (≈400-800 nm). The use of this range provides an opportunity to exploit an otherwise untapped medium that is used in human lighting. Most visible light communication systems constructed to date focus on using a broad visible band generated by phosphor-converted blue light emitting diodes, or by filtering to isolate the blue components from these sources. Multi-wavelength systems consider multiple wavelength bands that are combined to produce the desired spectrum realizing a desired color temperature and intensity. The use of multiple bands is also a form of wavelength-division multiplexing. In this paper, we investigate the relationships between the colors comprising the lighting source for a range of lighting states, the spectral separation of communication channels, the relative intensities required to realize a lighting states, how modulation can be most effectively mapped to the available color channels, and the design of an optical filtering approach to maximize SNR while minimizing crosstalk at the receiver. Simulation results based on currently available light emitting diode sources and novel optical filters are shown using orthogonal frequency division multiplexing models.

Keywords—Visible Light Communications (VLC), Optical Wireless Communications (OWC), Multiple Input Multiple Output (MIMO), Wavelength Division Multiplexing (WDM), Orthogonal Frequency Division Multiplexing (OFDM).

I. Introduction

There has been a rapid rise in use of networked portable computing devices in recent years. These devices are consuming increasingly more information in the form of multimedia streaming. The network infrastructure is strained to keep up with this increasing demand for wireless data creating the phenomenon of 'spectrum crunch'. Its effect can be seen in reduced quality of service at lower download speeds.

On the other hand, advances made by the solid state industry has created energy efficient illumination devices called light emitting diodes (LED). The intensity of radiant flux emitted by LEDs can be modulated at a high enough rate such that information transfer can be achieved at relatively high speeds while the intensity variations are invisible to human eye. One or more LEDs can be packaged together to form a 'luminaire' which under the above model serves the dual functionality of providing wireless network access and maintaining illumination. The additional downlink capacity provided by such 'smart' luminaires can help mitigate some of the aforementioned spectrum crunch.

A simple single input single output (SISO) VLC channel can be created by using an LED as a transmitter and a photodiode (PD) as a receiver. Information is modulated over the variations of the LED output flux. The PD produces an electrical signal proportional to the flux incident on it. This is also called intensity-modulation/direct-detection (IM/DD). The low modulation bandwidth of an illumination grade phosphor converted LED limits the achievable data rates. Research conducted in references cite tackle improving the bandwidth of LED based transmitters.

Another way of improving the capacity of a wireless channel is by using multiple transmitting and receiving elements in a multiple input multiple output (MIMO) configuration. A channel is created with multiple parallel links, each adding capacity to the channel. The parallel links can be established over dimensions such as space, time, frequency, wavelength, polarization, and others. Different types of MIMO systems cite have been reported in literature.

One type of an optical MIMO system is wavelength division multiplexed (WDM) VLC system. Different WDM system prototypes have been reported in literature cite. These describe an instance of a WDM system without analysis of the optimal operating point. In this work, we study the design of multi-wavelength visible light communication (VLC) systems under lighting constraints. We then analyze system performance variations when correlated color temperature (CCT) of illumination, transmitter spectral power distribution and receiver spectral transmittance are varied. The analysis provides an insight into optimal design criteria.

The following notations are used in this paper. Scalar values are represented in regular font. Vectors and matrices are represented in bold font. Conjugate transpose of $\mathbf{A}$ is represented by $\mathbf{A}^*$. Operators $:=$, $E[.]$, and $||.||$ represent definition, expectation, and euclidean norm respectively.

An introduction to optical multiple-input multiple-output (MIMO) systems is provided in Section II. Wavelength division multiplexing (WDM), a subset of optical MIMO systems, is introduced in Section III. Simulation and results are discussed in Section IV. Conclusions are then drawn in Section V.

II. Optical MIMO Channel

This section provides an introduction to an optical MIMO channel that can be established between multiple optical transmitting and receiving elements. Information over an optical channel is usually transmitted using intensity-modulation direct-detection (IM/DD). At the transmitting elements, information is modulated over the intensity of emitted light or radiant flux. Since output light intensity from a radiating source must be non-negative, the transmitted signals must be constrained to non-negative values. Multiple transmitting elements can be established over dimensions such as space, time, frequency, wavelength, polarization, and others. Each receiving element must produce an output electrical signal that is proportional to the radiant flux, from the dimension of interest, incident on it. Each parallel link must be sufficiently decorrelated with enough signal to interference and noise ratio (SINR) to meet the target bit error rate (BER).

A typical optical MIMO channel can be modeled as a linear time invariant system and be represented as

$$\mathbf{Y} = \mathbf{H}\mathbf{X} + \mathbf{W} \tag{1}$$

$\mathbf{X}$ is an N_{tx} dimensional vector. Each element of $\mathbf{X}$ represents the radiant flux emitted by each transmitting element. $\mathbf{Y}$ is an N_{rx} dimensional vector. Each element of $\mathbf{Y}$ represents the signal output from each receiving element. $\mathbf{H}$ is an $N_{rx} \times N_{tx}$ dimensional channel matrix. Each element $h_{ij} \in \mathbf{H}$; $i \in \{1, 2, \ldots, N_{rx}\}$, $j \in \{1, 2, \ldots, N_{tx}\}$ represents the conversion factor for signal output from the i^{th} receiving element when radiant flux from j^{th} transmitting element is incident on it after including the path losses. $\mathbf{W}$ is an N_{rx} dimensional noise vector. It is typically modeled as additive white Gaussian noise independent of transmitted vector $\mathbf{X}$ i.e. $\mathbf{W} \sim \mathcal{N}(\mathbf{0}, \sigma_n^2 \mathbf{I}_{N_{rx}})$.

The amount of radiant flux per solid angle emitted by the j^{th} transmitting element in a certain angular direction ϕ is given by the angular radiant intensity distribution. An LED's radiant intensity distribution is usually characterized by a Lambertian distribution given by

$$L_j(m, \phi) = \begin{cases} \frac{(m+1)}{2\pi} cos^m(\phi) & ; -\pi/2 \leq \phi \leq \pi/2 \\ 0 & ; \text{ else} \end{cases} \tag{2}$$

If Φ is the emission angle at which radiant intensity of a transmitting element is half its peak value (at $\psi = 0°$), the Lambertian order of that emission is $m = -ln(2)/ln(cos(\Phi_j))$.

A photodiode is a device that produces an electrical signal output that is proportional to the radiant flux incident on it. Photodiodes with larger active area can collect greater flux and thus output a larger signal. On the other hand, a large area photodiode offers a larger capacitance and thus reduces the signal bandwidth that can be received without distortion. Additionally, this also reduces the number of photodiodes that can be packed together to form a multi-element receiving array within a given area budget on a portable device. The photodiode effective area can be increased by using optics. Concentrator optics may be used for each photodiode element in non-imaging receiver arrays. The area gain provided by concentrator optics on the i^{th} receiving element is given by

$$G_i(\psi) = \begin{cases} \frac{\eta_i^2}{sin^2(\Psi_i)} & ; 0 \leq \psi \leq \Psi_i \leq \frac{\pi}{2} \\ 0 & ; \psi > \Psi_i \end{cases} \tag{3}$$

where ψ is the angle of incidence of the incident flux, η is the refractive index of the material that the optics are made of, and Ψ_i is the field of view of the i^{th} concentrator.

Optical filters may be used at the receiver to acquire only the wavelengths of interest while rejecting the ambient radiation. Depending on the type of filter used, its transmittance may be a function of the angle of incidence ψ. Let $T_i(\psi, \lambda)$ be the transmittance of the i^{th} optical filter. If $S(\lambda)$ is the normalized spectral power distribution (SPD) of incident radiation and $R_i(\lambda)$ is the responsivity of the i_{th} receiving photodiode, the effective responsivity of the i^{th} receiving element is given by

$$R_{e_i}(\psi) = G_i(\psi) \int_{\lambda_{min}}^{\lambda_{max}} S(\lambda) T_i(\psi, \lambda) R_i(\lambda) d\lambda \tag{4}$$

Let $\mathbf{d}_{ij}$ be the vector from receiving element i to transmitting element j. The distance between the two is then given by $||\mathbf{d}_{ij}||^2$. Let A_i be the active area of the photodiode. The channel gain from transmitting element j to receiving element i is given by

$$h_{ij} = L_{m_j}(\phi_{ij}) \frac{A_i}{||\mathbf{d}_{ij}||^2} cos(\psi_{ij}) R_{e_i}(\psi_{ij}) \tag{5}$$

where m_j is the Lambertian order of the j^{th} transmitting element, and ϕ_{ij} and ψ_{ij} are the angles subtended between vector $\mathbf{d}_{ij}$ and surface normals respectively of the j^{th} transmitting and i^{th} receiving elements.

Ambient light incident on a photodiode generates shot noise. Let $P_a(\lambda)$ be SPD of isotropic ambient light. This would generate shot noise in the i^{th} receiving element with variance

$$\sigma_{sh_i}^2 = \frac{2qA_iG_i(\Psi_i)}{\Psi_i} \int_{\lambda_{min}}^{\lambda_{max}} \int_0^{\Psi_i} P_a(\lambda) T_i(\psi, \lambda) R_i(\lambda) d\psi d\lambda \tag{6}$$

where $q = 1.6 \times 10^{-19}$ C is the charge of an electron. Shot noise statistics are typically modeled as a Poisson distribution.

A trans-impedance amplifier (TIA) is most often used as the first stage amplifier. Thermal noise is the most dominant component of TIA electrical noise. The thermal noise variance in the i^{th} receiving element is given by

$$\sigma_{th_i}^2 = \frac{4kT_i}{R_{f_i}} \tag{7}$$

where constant k is Boltzmann constant, T_i is the absolute temperature and R_{f_i} is the TIA feedback resistance. Thermal noise statistics are typically modeled as a Gaussian distribution.

Total input referred noise variance is usually approximated as the sum of shot noise variance and thermal noise variance. For sake of mathematical simplicity, total noise is assumed to have Gaussian statistics with mean 0 and variance $\sigma_{n_i}^2 = \sigma_{sh_i}^2 + \sigma_{th_i}^2$.

In VLC, transmitting elements perform dual function of providing wireless data transmission while maintaining illumination levels. To perform a fair comparison between different modulation systems operating at same illumination levels needs a different definition of SNR. In this work, SNR is

defined as the ratio of the average transmitted electrical power to noise power and is similar as in [1].

$$SNR_{avg}^{tx} = \frac{(hP_{avg}^{tx})^2}{\sigma_n^2} \tag{8}$$

where P_{avg}^{tx} is the average radiant flux emitted by a transmitter, h is the optical to electrical conversion factor $(AW^{-1}\Omega^{-2})$ and σ_n^2 is the noise power.

III. Wavelength Division Multiplexing

There are different types of light sources that are used to provide illumination in indoor spaces. Incandescent light sources have been the most popular. They have excellent color rendition. However, since most of the energy consumed is converted to heat or produces invisible radiation, they are very power inefficient. Fluorescent light sources excite mercury atoms to produce ultraviolet radiation which then excites a phosphor coating to produce visible light. Fluorescent sources are much more energy efficient than incandescent sources and their output spectrum can be tailored by using different phosphor compositions. Both, incandescent and fluorescent sources produce a broad spectrum of light whose correlated color temperature (CCT) usually lies close to the black body radiation curve.

With recent advances in solid state technology, light emitting diodes (LEDs) have emerged as the most energy efficient sources for illumination. There are two distinct methods for producing 'white' light using LEDs. One way is to use a blue LED with a phosphor coated encapsulant that produces yellow light when excited. On emission, the blue and the yellow combine to produce white light. Different phosphors can be used to mix different ratios of blue and yellow to generate different 'white' CCTs. Alternative way is to use LEDs that emit different narrow-band spectrum and combine the emissions in different ratios to produce different colors for illumination including the shades of 'white' on the black body radiation curve. Recent work by XYZ et al explores using different colored lasers to provide good quality illumination.

The ability to combine multiple narrow band sources to generate white light also provides the benefit of being able to transmit concurrent information streams over different color groups; thus enabling wavelength division multiplexing (WDM). The performance of a multi-colored VLC system depends on a number of parameters including SPD of the transmitting elements, illumination color, filter transmission function, and receiver responsivity.

Lasers and LEDs produce a much smaller SPD width as compared to incandescent and fluorescent sources and are thus preferable for WDM. LED emission can be modeled with a Gaussian distribution (9a) while laser emission can be modeled with a Lorentzian distribution (9b). Equations in (9) model emission spectra for the j^{th} transmitting element.

$$S_j(\lambda) = \frac{1}{\sqrt{2\pi\sigma_j^2}} exp\left[-\frac{(\lambda-\lambda_j)^2}{2\sigma_j^2}\right] \tag{9a}$$

$$S_j(\lambda) = \frac{1}{\pi}\frac{0.5\Gamma_j}{(\lambda-\lambda_j)^2 + (0.5\Gamma_j)^2} \tag{9b}$$

where λ_j is the dominant wavelength of emission, σ_j is the measure of deviation from the dominant wavelength for the Gaussian model, and Γ_j is the full width at half maximum (FWHM) from the dominant wavelength for the Lorentzian model. At small SPD width, most of the optical power is emitted at the dominant wavelength. At larger SPD widths the optical power is spread across a larger wavelength range and starts overlapping across different transmitting elements, thus causing interference.

To generate white light $W(\lambda)$, emissions from different transmitting elements are weighted by factor t_j before being mixed together. The resulting spectrum is given by

$$W(\lambda) = \sum_{j=1}^{N_{tx}} t_j S_j(\lambda) \tag{10}$$

The *commission internationale de l'éclairage* (CIE) specified the CIE 1931 XYZ color space. It maps an SPD to a color representation as sensed by the human eye. The standard defines three color matching functions $\bar{x}(\lambda)$, $\bar{y}(\lambda)$, and $\bar{z}(\lambda)$ as shown in figure. The tristimulus values for the XYZ primaries are given by

$$X_W = \int_{\lambda_{min}}^{\lambda_{max}} W(\lambda)x_c(\lambda)d\lambda \tag{11a}$$

$$Y_W = \int_{\lambda_{min}}^{\lambda_{max}} W(\lambda)y_c(\lambda)d\lambda \tag{11b}$$

$$Z_W = \int_{\lambda_{min}}^{\lambda_{max}} W(\lambda)z_c(\lambda)d\lambda \tag{11c}$$

A color can be expressed in terms of its chromaticity and luminance. Chromaticity coordinates capture the hue and saturation of the color while luminance captures the amount of light in the color. The chromaticity coordinates for the SPD can be then be computed from the tristimulus values as

$$\begin{bmatrix} x \\ y \end{bmatrix} = \frac{1}{X_W + Y_W + Z_W}\begin{bmatrix} X_W \\ Y_W \end{bmatrix} \tag{12}$$

The spectral radiance of a black body heated to temperature T as stated by Planck's law is given by

$$S(\lambda) = \frac{2hc^2}{\lambda^5\left[exp\left(\frac{hc}{\lambda kT}\right) - 1\right]} \tag{13}$$

where h is the Planck's constant, c is speed of light, and k is Boltzmann's constant. Replacing $W(\lambda) = S(\lambda)$ in Eq.(11) and then from Eq.(12) we obtain the CIE 1931 XYZ chromaticity values $[x, y]$ associated with a black body heated to temperature T. In this context T is also known as the correlated color temperature (CCT) for color represented by $[x, y]$. Note that two different SPDs can generate the same chromaticity coordinates. This is due to the principle of metamerism.

Traditionally luminaires have been specified to generate a certain CCT with colors are lower temperature appearing (ironically) warm than those at higher temperatures. It is practical to generate colors off the black body radiation curve using different colored lasers and LEDs. However for this analysis, we shall stick to colors generated on the black body radiation curve. As the CCT changes from a lower value

to a higher value, the optical power available to transmit information on any color channel varies thus affecting the overall communication performance.

Optical filters can be manufactured to permit narrow bandpass filtering with nanometer precision using plasmonics. Broad bandpass optical filters that make use of interference are widely available. The transmittance of these filters can be modeled as Lorentzian functions of wavelength. The choice of the filter FWHM is a tradeoff to collect the maximum signal while rejecting interference and background illumination.

Responsivity of the receiving elements also affects the aggregate system performance. It depends on the quantum efficiency of the material of sensor and is given by

$$R(\lambda) = \frac{\eta\lambda}{1240} \tag{14}$$

where η is the quantum efficiency of the material, and λ is wavelength of interest. For equal signal radiant flux, signals that span wavelength ranges with lower responsivity will perform poorly as compared to the rest.

IV. Simulation and Results

We wish to study how the choice of design parameters like transmitter SPD, filter transmittance and CCT affect the performance of a multi-colored VLC system. We chose three transmitting elements with dominant wavelengths at red (627 nm), green (530 nm) and blue (470 nm). These are modeled to have Gaussian emission spectrum. We also seek to achieve CCT range of [2500 7000] K. Normalized SPDs to achieve this range of CCTs with different transmitting SPD widths is illustrated in figure. For all CCTs, a total received illumination of 400 lx is maintained.

Unique $t_R : t_G : t_B$ ratios are generated after varying the tristimulus values in the range [0 1] in 0.1 unit steps. By substituting these values in Eq.(10)-Eq.(12), we calculate chromaticity coordinates for resulting SPDs. An initial characterization step generates a pre-populated table consisting of the tristimulus values and corresponding chromaticity coordinates. As the CCT is varied, the chromaticity coordinates are computed as shown in Section III. From the pre-computed table, the tristimulus values that achieve the closest chromaticity are selected. The SPD is then scaled to achieve target illumination (400 lx) at the receiver.

Optical filter's passband can be designed to center on the transmitting element's dominant wavelength. Optical filters for the simulation are modeled to have Lorentzian transmittance with ideal value 1 at the dominant red, green and blue wavelengths mentioned above. Filter transmittance as a function of wavelength is illustrated in figure. Filter FWHM considered for the analysis lie in [1 150] nm range.

We assume the receiver sensor to be made of silicon. The assumed quantum efficiencies and responsivity of the sensor is illustrated in figure. The responsivity near the blue wavelength is about 0.1 $A.W^{-1}$ and increases steadily to about 0.4 $A.W^{-1}$ near the red before rapidly reducing as the energy of the incident photon approaches the bandgap energy of silicon.

Having established $N_{tx} = 3$ transmitting and $N_{rx} = 3$ receiving elements, the 3×3 channel matrix $\mathbf{H}$ can be computed as in Section II. To analyze the system performance, a random bit stream is generated. Bits for each link are then framed using ACO-OFDM and DCO-OFDM using 64 subcarriers and 64-QAM and 32-QAM modulation respectively. The DC level on each link is set to ensure the desired CCT is achieved at the illumination levels. This generates the transmit vector $\mathbf{X}$. Noise is then added to the transmitted vector. $\mathbf{Y}$ then collects the received signal and the added noise and interference. The signal is estimated and decoded. Bit error rate (BER) is then calculated by comparing the transmit and estimated bit streams.

The change in performance of the red, green and blue links as the CCT is varied is shown in figure. At 2500K, the SPD has a greater contribution from red, then green and then blue. Thus the red link achieves target BER at lower signal power. As the CCT increases from 2500K to 7000K, the red signal power decreases, green signal power remains similar and the blue signal power increases. The performance of the red link starts degrading, while that of the green remains relatively unchanged while that of the blue improves with increase in CCT.

The change in performance of the red, green and blue links as the transmitting element SPD width is varied is shown in figure. As the SPD width is increased, the performance of all three links degrade. This can be attributed to two factors. Initially, as the signal power is distributed across a larger wavelength range, with the filter transmittance function remaining the same, increasingly more signal gets rejected by the filter. This the receiver collects a smaller fraction of the signal power, degrading the performance. Secondly, as the individual SPDs become wide enough, they start overlapping and causing ICI. The effect of ICI is more pronounced on the green channel because it gets interference from both, red and blue. Thus transmitting elements with narrower emission spectra perform better.

The change in performance of the red, green and blue links as the receiving element filter FWHM is varied is shown in figure. As the filter FWHM is increased from 0 nm to 250 nm, initially the system performance improves with the best performance for each link within the 40 nm - 80 nm range. At the lower FWHM ranges, the filters transmit a smaller fraction of the signal to the sensors and thus performance is limited by the amount of signal power collected for each link. At higher FWHM ranges, along with additional signal, the filters permit increasingly more ambient light and signals from neighboring channels. This adds additional noise and interference to the link, thus degrading the performance. For the specified multi-colored system, filter FWHM within [40 80]nm seems optimal.

V. Conclusion

VI. Acknowledgement

This work was supported by the Engineering Research Centers Program of the National Science Foundation under NSF Cooperative Agreement No. EEC-0812056.

References

[1] T. Fath and H. Haas, "Performance comparison of mimo techniques for optical wireless communications in indoor environments," *Communications, IEEE Transactions on*, vol. 61, no. 2, pp. 733–742, 2013.

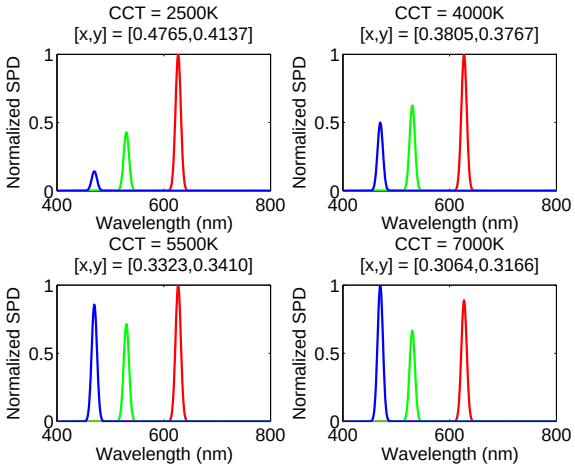

Fig. 1. Transmitting Element Normalized Spectral Power Distribution

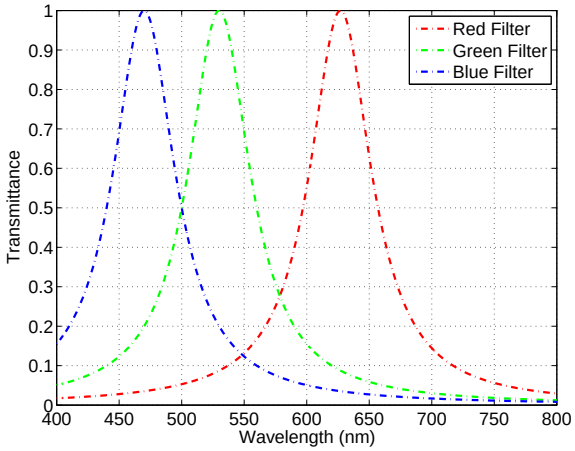

Fig. 2. Filter Transmittance (FWHM=60nm)

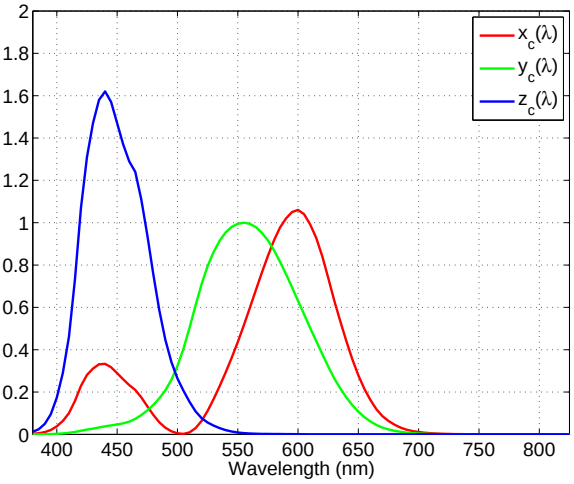

Fig. 3. CIE XYZ 1931 Model Color Matching Functions

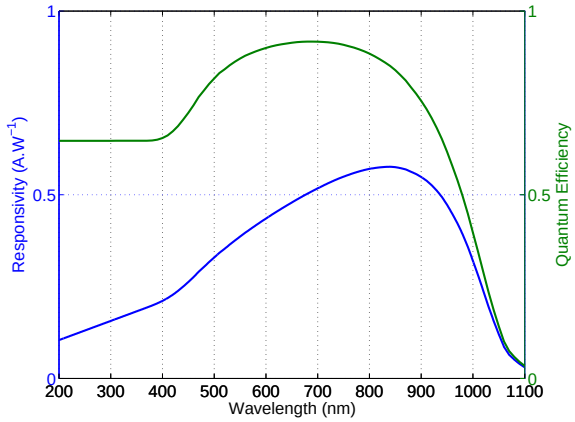

Fig. 4. Receiver Responsivity

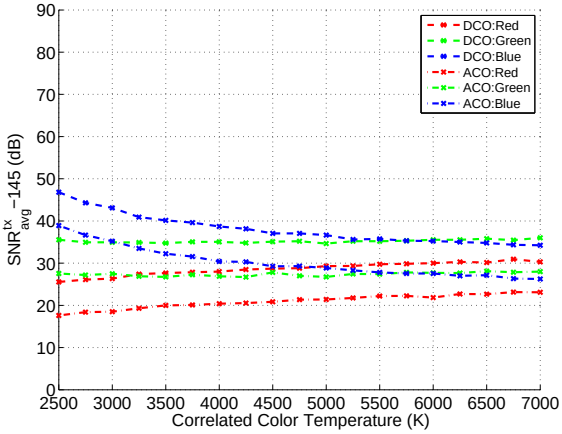

Fig. 5. SNR_{avg}^{tx} vs Corelated Color Temperature

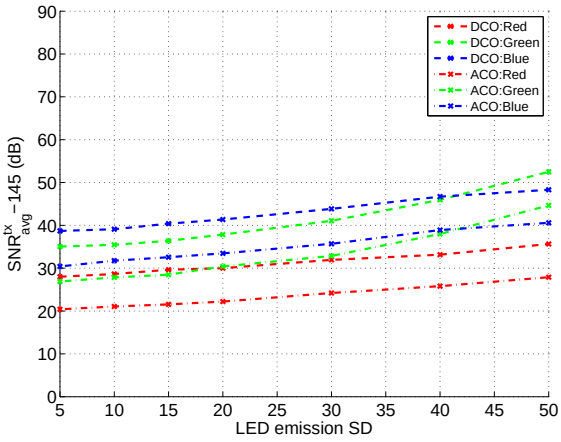

Fig. 6. SNR_{avg}^{tx} vs Transmitting Element Spectral Power Distribution Width

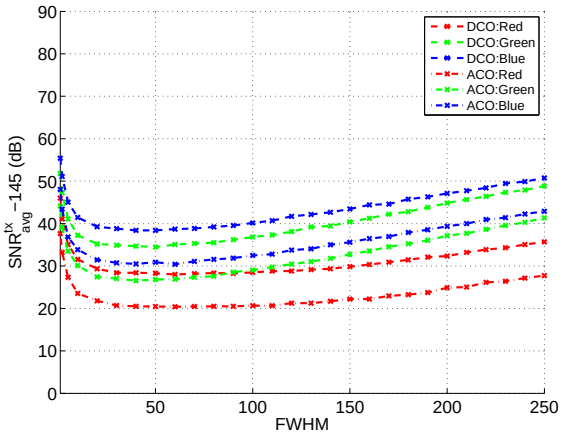

Fig. 7. SNR_{avg}^{tx} vs Filter Full Width at Half Maximum